Ann. Geophys. Discuss., https://doi.org/10.5194/angeo-2018-48
Manuscript under review for journal Ann. Geophys.
Discussion started: 5 June 2018

Annales Geophysicae Discussions
Open Access
EGU

Variability of TEC and improvement of performance of the IRI model over Ethiopia during the high solar activity phase

Yekoye Asmare Tariku

Department of Space Science and Research Application Development, Ethiopian Space Science and Technology Institute, Addis Ababa, Ethiopia

* Corresponding author. Tel. +251912799754

Email_address:yekoye2002@gmail.com (Yekoye Asmare)

Abstract

This paper discusses the monthly and seasonal variation of the total electron content (TEC) and the improvement of performance of the IRI model in estimating TEC over Ethiopia during the solar maximum (2013-2016) phase employing GPS TEC data inferred from the GPS receivers installed at different regions of Ethiopia. The results reveal that both the measured and modeled seasonal diurnal VTEC values start increasing at 03:00 UT (06:00 LT) and attain their peak values (mostly in the time interval of 09:00-13:00 UT or 12:00-16:00 LT). Moreover, both the arithmetic mean measured and modeled VTEC values, generally, show maximum and minimum values in the equinoctial and June solstice months, respectively. The results also show that, even though overestimation of the modeled VTEC has been observed on most of the hours, the model is generally good to estimate both the monthly and seasonal diurnal hourly VTEC values, especially in the early morning hours (00:00-03:00 UT or 03:00-06:00 LT). Moreover, the overall

Ann. Geophys. Discuss., https://doi.org/10.5194/angeo-2018-48
Manuscript under review for journal Ann. Geophys.
Discussion started: 5 June 2018

results show that using NeQuick option for the topside electron density is the best option in estimating the TEC variation. It has also been shown that the model does not show a good improvement on its performance in estimating both the monthly and seasonal hourly and arithmetic mean VTEC values. Moreover, the model does not respond to the effects resulting from storm.

Key words: GPS-VTEC; IRI- VTEC; GPS signal, solar maximum

1. Introduction

The energy transferred from the sun causes atoms and molecules existing in the atmosphere to undergo chemical reactions and become ionized (Kelley, 2009). This ionized and conductive region of Earth's atmosphere, extending from about 50 to 1000 km and possessing free electrons and positive ions generally in equal numbers in a medium that is electrically neutral, is termed as ionospher. The existence of these ions (plasma) in the ionosphere results in the possibility of radio communications over large distance by making use of one or more ionospheric reflections (Hunsucker and Hargreaves, 2003).

On the other hand, the ionosphere affects the electromagnetic waves that pass through it by inducing additional transmission time delay (Gao and Liu, 2002). Because of its dispersive character, electromagnetic signals (such as GPS signals) experience time delay (modulated codes) and advance (carrier phase) as they propagate through the ionosphere. This delay is directly proportional to the integral number of electrons in a unit cross-sectional area (usually referred to as total electron content, TEC) along the signal path extending from the satellite to the receiver on the ground, and inversely proportional to the square of the frequency of propagation (Hofmann-Wellenhof et al., 1992; Misra and Enge, 2006). The dispersive ionosphere introduces

Ann. Geophys. Discuss., https://doi.org/10.5194/angeo-2018-48
Manuscript under review for journal Ann. Geophys.
Discussion started: 5 June 2018

a time delay in the 1.57542 GHz (L1) and 1.22760 GHz (L2) simultaneous transmissions from GPS satellites orbiting at 20,200 km (Hansen et al., 2000). The relative ionospheric delay of the two signals is proportional to the TEC. Time delay measurements of L1 and L2 frequencies can, therefore, be converted to TEC along the ray path from the receiver to the satellite (Lanyi and Roth, 1988). The GPS signals traverses the ionosphere carrying signatures of the dynamic medium and thus offers opportunities for ionospheric research. As a result, global and regional maps of ionospheric TEC can be produced using data from the worldwide network of the International GPS Service (Lanyi and Roth, 1988). The availability of TEC measurements is also important to the development of ionospheric models such as the International Reference Ionosphere, IRI (Bilitza, 2001). The International Reference Ionosphere (IRI) is an international project sponsored by the Committee on Space Research (COSPAR) and the International Union on Radio Science (URSI).

Using the GPS satellites and the IRI model, there have been so far several researches conducted globally in connection with the TEC variability and performance of the model over equatorial and low latitude regions. Based on the findings, the researchers have put their own views concerning the TEC variation and the prediction performance of different versions of the model. Ezquer et al. (2014), for instance, noted that IRI 2012 predictions show significant deviations from experimental values during the period of 2008-2009 for a station placed at the southern crest of the equatorial anomaly in the American region. Olwendo et al. (2012a) also noted that seasonal average IRI 2007 TEC values were higher than the GPS-TEC data for the period of 2009-2011 over different regions in Kenya. In addition, Olwendo et al. (2012b) reported that the IRI 2007 TEC is too high for all seasons except for the March equinox (where there seems to be good agreement between observation and model) during the lowest solar

activity phase (2009-2010). The report of Kumar (2016) on the validation of the IRI 2012 models for the global equatorial region also showed that the IRI 2012 model generally overestimated the observed VTEC over equatorial regions during the solar minimum year (2009) and solar maximum (2012) phases. Abdu et al. (1996); Kakinami et al. (2012); Kumar et al. (2015) attempted to describe the model's capacity to estimate the TEC using different versions of the model. Asmare et al. (2014) and Tariku, 2015a and Tariku, 2015b also attempted to see patterns in both the measured and modeled VTEC variations during the low and high solar activity phases employing different GPS stations and IRI 2012 model at various regions of Ethiopia. Asmare et al. (2014), for instance, showed that the model entirely overestimated both monthly and seasonal VTEC values during phases of low solar activity. In addition, the model performance in estimating diurnal VTEC variations was found to be better during low solar activity phases than during high solar activity phases. In addition, the highest and the lowest values of the VTEC are observed in the equinoctial and the June solstice months, respectively during both the low and high solar activity phases.

Thus, this study is mainly important to observe the TEC variation and the improvement of performance of the IRI model in estimating the TEC variation over low latitude African regions during the high solar activity phase (2013-2016) employing the GPS VTEC data inferred from different regions of Ethiopia. This is because the TEC is the major parameter that can largely affect radio wave propagation in the ionosphere. Consequently, for a better radio wave propagation which can foster Earth-to-space communication, the TEC in the ionosphere has to be studied and its effects on the signal propagated through the ionosphere must be identified. In addition, for a better improvement of the IRI model in estimating the variation of TEC, its performance has to be continuously tested, especially over the equatorial and low latitude

Ann. Geophys. Discuss., https://doi.org/10.5194/angeo-2018-48
Manuscript under review for journal Ann. Geophys.
Discussion started: 5 June 2018

regions, where the dynamics of the ionosphere is very complex. To observe the TEC variation and improvement of performance of the IRI model in estimating the TEC variation the latest versions (IRI 2007, IRI 2012 and IRI 2016) with NeQuick option for the topside electron density during the solar maximum phase have been considered. This is conducted to choose and use the best version of the model in estimating the TEC variability in some occasions when the GPS TEC data are scarcely available in the receiver. The prediction performance of the model has been tested by comparing the modeled TEC values with the GPS-TEC values recorded in the receivers.

2. Data description and analysis method

2.1. TEC from dual frequency GPS receiver

As different studies (e.g. Ciraolo et al., 2007; Mannucci et al., 1998) show that the GPS measurements are used to estimate the TEC along a ray path between a GPS satellite and receiver on the ground. These GPS measurements can be recorded using either single or dual frequency GPS receivers. However, to eliminate ionospheric errors in the estimation of TEC dual frequency receivers are better (Klobuchar, 1996). Moreover, by computing the differential phases of the code and carrier phase measurements, dual frequency GPS receivers can provide integral information about the ionosphere and plasma sphere (Ciraolo et al., 2007; Nahavandchi and Soltanpour, 2008). Hence, in this paper, the GPS-TEC data have been obtained from dual frequency receiver using pseudo-range and carrier phase measurements. The TEC inferred from the pseudo-range (P) measurement is given by:

Ann. Geophys. Discuss., https://doi.org/10.5194/angeo-2018-48
Manuscript under review for journal Ann. Geophys.
Discussion started: 5 June 2018

$$TEC_P = \frac{1}{40.3}\left[\frac{f_1^{\,2} f_2^{\,2}}{f_1^{\,2} - f_2^{\,2}}\right](P_2 - P_1). \quad \textbf{(1)}$$

Similarly, the TEC from carrier phase measurement (Φ) is given as

$$TEC_\Phi = \frac{1}{40.3}\left[\frac{f_1^{\,2} f_2^{\,2}}{f_1^{\,2} - f_2^{\,2}}\right](\Phi_1 - \Phi_2), \quad \textbf{(2)}$$

where f_1 and f_2 can be related with the fundamental frequency, $f_o = 10.23MHz$

$$\begin{aligned} f_1 &= 154\, f_o = 1575.42MHz, \\ f_2 &= 120\, f_o = 1227.60MHz. \end{aligned} \quad \textbf{(3)}$$

As shown above, by cross correlating the f_1 and f_2 modulated carrier signals which are generally assumed to travel along the same path through the ionosphere, the GPS receiver obtains the time delay of the code and the carrier phase difference. As the TEC obtained from code pseudo-range measurements is free of ambiguity, but with relatively much noise; and the TEC obtained from carrier phase measurements has relatively less noise, but is ambiguous, linearly combining both code pseudo-range and carrier phase measurements for the same satellite pass is supposed to increase the accuracy of TEC (Klobuchar et al., 1996; Gao and Liu, 2002). To better characterize the TEC over a given receiver position and see the overall ionization of the Earth's ionosphere, the slant TEC (STEC) must be converted into equivalent vertical TEC (VTEC) at the mean ionospheric height, h_m=350 km (Mannucci et al., 1998; Norsuzila et al., 2008, 2009). Hence, the relationship between STEC and VTEC in terms of the zenith angle χ' at the Ionospheric Piercing Point (IPP) and the zenith angle χ at the receiver position can be given by:

$$VTEC = STEC(\cos\chi'), \quad \textbf{(4)}$$

Ann. Geophys. Discuss., https://doi.org/10.5194/angeo-2018-48
Manuscript under review for journal Ann. Geophys.
Discussion started: 5 June 2018

where, .

$$\chi' = \arcsin[\frac{R_e}{R_e + h_m}\sin\chi]. \quad \textbf{(5)}$$

Substituting equation (5) into equation (4) and rearranging, we get

$$VTEC = STEC\left\{\cos\left[\arcsin\left(\frac{R_e}{R_e + h_m}\sin\chi\right)\right]\right\}. \quad \textbf{(6)}$$

Here, R_e is the radius of the Earth in kilometers.

2.2. TEC from the International Reference Ionosphere (IRI) model

The International Reference Ionosphere (IRI) is an international empirical standard model used for the specification of ionospheric parameters. The model provides average values of electron density, electron content, electron and ion temperature, and ion composition as a function of height, location, local time, and sunspot number for magnetically quiet conditions (Bilitza, 2001; Bilitza et al., 2014; Bilitza et al., 2017). To enhance the capacity of the model, improvements have been made through the ingestion of all worldwide available data from ground-based as well as satellite observations. As a result, a new version of the model (IRI 2016) has been released in 2017 by incorporating some new input parameters that are supposed to increase its capacity. The IRI 2016 model includes two new model options for the F2-peak height hmF2 and a better representation of topside ion densities at very low and high solar activities. The two new options are used in modeling *hmf2* directly and no longer through its relationship to the propagation factor *M(3000)F2*. Thus, the new model options enable the IRI 2016 model to predict evening peaks that was not possible in the old versions. In addition, the improvement of the ion composition model in the topside ionosphere can lower the transition

Ann. Geophys. Discuss., https://doi.org/10.5194/angeo-2018-48
Manuscript under review for journal Ann. Geophys.
Discussion started: 5 June 2018

height from close to 1000 km down to almost 600 km in the new version of the model. A number of smaller changes have also been made concerning the use of solar indices and the speed-up of the computer program (Bilitza et al., 2017). For a given location, time and date, like the previous versions of the model, IRI-2016 model provides the monthly averages of ionospheric parameters (such as TEC) in the altitude range from about 50–2000 km (Bilitza et al., 2017; http://IRImodel.org.). For more information, see the model web site **(**http://omniweb.gsfc.nasa.gov/vitmo/iri-vitmo.html**)** that was accessed for the period of 25-30/01/2018.

2.3. Data sources and method of analysis

The data required for both the experimental and model were obtained from Ethiopian regions shown in Figure 1 during the solar maximum (2013-2016) phase. Table 1 also shows the GPS receiver locations used for the study. The raw GPS data for the described station were obtained from the University NAVSTAR Consortium (UNAVCO web site, http://www.unavco.org/). The data gained from this web site have two forms: observation and navigation data in which both of them are zipped. To use the data for the desired purpose, the GG software (GPS-TEC calibrating software) was used to process the required data in five minutes interval and an elevation cut-off 10^{o} (see Ciraolo, et al., 2007).

To get the required results, the corresponding modeled VTEC values were inferred from the latest versions of the model (IRI 2007, IRI 2012 and IRI 2016) that include some latest input parameters which are supposed to improve the capacity of the model in estimating ionospheric parameters. The online IRI versions of the model were obtained from http://omniweb.gsfc.nasa.vitmo.html. To get the VTEC values, the year, date, month, location,

Ann. Geophys. Discuss., https://doi.org/10.5194/angeo-2018-48
Manuscript under review for journal Ann. Geophys.
Discussion started: 5 June 2018

the hour profile, the upper boundary altitude (2000 km), daily sunspot number and F10.7 radio flux, topside electron density options (NeQuick, IRI01-corr, IRI2001), CCIR for F peak model, and ABT-2009 for bottomside thickness option were used as the input parameters,.

In order to observe the pattern of the hour-to-hour variability of VTEC, the mean monthly and seasonal hourly GPS TEC and the corresponding IRI TEC data have been used during the period of 2013-2016. To see the monthly and seasonal arithmetic mean VTEC variation and the model performance, the hour-to-hour measured and modeled VTEC values have been correspondingly added and averaged for the whole days in each month and season. The seasons could be classified as December solstice (November, December and January), March equinox (February, March and April), June solstice (May, June and July) and September equinox (August, September and October). For a better understanding on the performance of the model, the absolute differences between the monthly and seasonal GPS VTEC and the corresponding IRI VTEC values have been determined. The differences have been calculated by subtracting the experimental VTEC values from the model. In order to clearly see the validation of the model, the absolute differences between the IRI VTEC and GPS VTEC in all the monthly and seasonal variations were determined. In addition, the percentage differences between the IRI VTEC and GPS VTEC for the arithmetic monthly and seasonal VTEC variations have also determined.

3. Results and discussion

3.1. Diurnal monthly and seasonal variation of VTEC and performance of the IRI model

The diurnal monthly and seasonal VTEC variation results are displayed in Figs 2-7. The results reveal that, almost both the monthly diurnal GPS VTEC and IRI VTEC values start increasing at 03:00 UT (06:00 LT) and attain their peak values in the daytime hours (especially in the time

Ann. Geophys. Discuss., https://doi.org/10.5194/angeo-2018-48
Manuscript under review for journal Ann. Geophys.
Discussion started: 5 June 2018

interval of 09:00-13:00 UT or 12:00-16:00 LT) due to enhancement of ionization during the described time; while their values start decreasing in the nighttime hours and become minimum after midnight hours (on average at 03:00 UT or 06:00 LT) as shown in figures 2-7. Moreover, in some hours, the modeled VTEC values are found to be in a good agreement with the measured (GPS VTEC) values, especially in the nighttime hours (00:00-03:00 UT or 03:00-06:00 LT). Moreover, the model is found to underestimate the VTEC values during the daytime hours (09:00-13:00 UT or 12:00-16:00 LT). The mismodelings observed in both cases may be due to the difference in the model and experimental slab-thickness as noted by different findings (e.g. Nigussie et al., 2013; Rios et al., 2007). For instance, Rios et al. (2007) using the IRI 2001 model, showed that IRI predicted slab thickness is higher than the measured values except between (10:00-14:00 LT) which can attribute to VTEC fluctuations in similar trend. This is almost consistent with the result determined in this work. Using IRI 2007 model, Nigussie et al. (2013) also suggested similar possible reason for the discrepancy between the model and the experimental VTEC values. It could also be resulting from poor estimation of the hmF2 and foF2 from the coefficients, which in turn may result in poor estimation of VTEC by the IRI model (e.g. Chakraborty et al., 2014; Kumar et al, 2015). The underestimation of the IRI VTEC values by the GPS VTEC values may also attribute to the enhancement of the plasmaspheric electron content above 2000 kms during the daytime hours.

Moreover, the maximum peak of both the measured and modeled VTEC values are generally observed in the equinoctial months; while, the minimum peak values are observed in the June solstice months (see Fig. 2-7). For instance, over Arba Minch station (see Figs. 2 and 3), the highest and lowest peak measured monthly VTEC values of about 80 and 40 TECU are observed in March and July, respectively. Similarly, the highest and lowest peak modeled

Ann. Geophys. Discuss., https://doi.org/10.5194/angeo-2018-48
Manuscript under review for journal Ann. Geophys.
Discussion started: 5 June 2018

seasonal VTEC values of about 55 and 41 TECU are observed in April and July, respectively in using IRI 2007 model with NeQuick option for the topside electron density.

The seasonal diurnal VTEC values generally follow the pattern of the diurnal monthly VTEC values with the lowest and highest values being observed at about 03:00 UT (06:00LT) and in the time interval of about 09:00–13:00 UT (12:00–16:00 LT), respectively (see Fig. 4-7). In addition, the highest and lowest peak measured seasonal VTEC values of about 80 and 50 TECU are observed in the March equinox and June solstice, respectively. The highest and lowest peak modeled seasonal VTEC values of about 54 and 43 TECU are observed in the March equinox and June solstice, respectively when using IRI 2007 model with NeQuick option for the topside electron density over Arba Minch station (see Fig. 6). In addition, in using IRI-2012 model with IRI-2001 option for the topside electron density, the highest and lowest peak measured seasonal VTEC values of about 70 and 40 TECU are observed in the March equinox and June solstice, respectively over Ambo station in 2014. Similarly, the highest and lowest peak modeled seasonal VTEC values of about 74 and 60 TECU are observed in the March equinox and June solstice, respectively in 2014 when using the same version of the model (IRI 2012) with IRI-2001 option (see Fig. 5).

It is known that, in general, electron population in the ionosphere is mainly controlled by solar photo-ionization and recombination processes (Wu et al., 2004). Thus, for the equinoctial months, as the subsolar point is around the equator where the east ward electrojet associated electric field is often largest, it would be speculated that the peak photoelectron abundance and intense eastward electric field will be set up in the described region. On the contrary, for solstice months photoelectrons at the equator decrease as the sub solar point moves to higher latitudes. Moreover, the change of direction of neutral wind may account for the highest VTEC values in

Ann. Geophys. Discuss., https://doi.org/10.5194/angeo-2018-48
Manuscript under review for journal Ann. Geophys.
Discussion started: 5 June 2018

246 the equinoctial months and lowest values in the June solstice months. A meridional component
247 of neutral wind blows from the summer to the winter hemisphere that is able to reduce the
248 ionization crest value during summer solstice as it blows in an opposite direction to the plasma
249 diffusion process originating from the magnetic equator. Thus, in equinoxes meridional winds
250 blowing from the equator to polar regions may attribute to a high ionization crest value. Hence, a
251 seasonal effect on the crest should be expected with the crest maximum at the equinoxes and
252 minimum in the summer season or June solstice (Bhuyan and Borah, 2007; Wu et al., 2004),
253 which is consistent with the result of this work.
254
255 3.2. *Arithmetic mean of monthly and seasonal variation of VTEC and performance of the IRI*
256 *model*
257 To visualize the monthly and seasonal VTEC variations, the arithmetic mean hourly
258 measured (GPS VTEC) and modeled (IRI VTEC) values obtained during the period of the high
259 solar activity phase (2013-2016) have been considered. The results are displayed in Figure 8-11.
260 The results show that both the measured and the modeled mean hourly VTEC have the highest
261 and lowest values in the equinoctial and June solstice months. For example, the highest and
262 lowest GPS arithmetic mean monthly VTEC values of about 38 and 18 TECU are observed in
263 April and July, respectively in the year 2014 over Ambo station. Similarly, the highest and
264 lowest modeled arithmetic mean monthly VTEC values of about 50 and 35 TECU are observed
265 in October and July, respectively in the year 2013 when using IRI-2001 option for the topside
266 electron density (see the left top panel of Fig. 9). The seasonal GPS arithmetic mean VTEC
267 variation also shows the highest and lowest values of about 37 and 21 TECU in the March
268 equinox and June solstice, respectively in 2014. In the same way, the highest and lowest seasonal

Ann. Geophys. Discuss., https://doi.org/10.5194/angeo-2018-48
Manuscript under review for journal Ann. Geophys.
Discussion started: 5 June 2018

modeled arithmetic mean VTEC values of about 44 and 39 TECU are observed in the March equinox and June solstice, respectively in 2013 when using IRI 2012 model with IRI-2001 option (see the bottom left panel of Fig. 8). In addition, the highest and lowest GPS arithmetic mean monthly VTEC values of about 37 and 17 TECU are observed in March and July, respectively over Arba Minch station in 2015 (see the top left panels of Fig. 10). Similarly, the highest and lowest modeled arithmetic mean monthly VTEC values of about 34 and 24 TECU are observed in April and July, respectively when using IRI 2016 model with NeQuick option for the topside electron density. The seasonal GPS arithmetic mean VTEC variation also shows the highest and lowest values of about 36 and 23 TECU in the March equinox and June solstice, respectively over Arba Minch station in 2015. In the same way, the highest and lowest seasonal modeled arithmetic mean VTEC values of about 32 and 24 TECU are observed in the March equinox and June solstice, respectively when using IRI 2007 model (see the left bottom panels of Fig. 10). In general, using the IRI 2016 model shows highest overestimation of the VTEC as compared to others (IRI 2007 and IRI 2012). For instance, the highest monthly and seasonal deviations of about 25% and 20% are observed between the modeled and corresponding measured values in September and the June solstice, respectively in using IRI 2016 model (see the bottom right panels of Fig. 10).

3.3 Storm Time VTEC Variation and Performance of the IRI Model

To see the VTEC variation and performance of the IRI model during storm time condition, the magnetic storm day (with Dst index about -222nT) which occurred on March 17, 2015 as observed over Arba Minch station was considered. To better see the effect of the storm on the GPS VTEC and IRI VTEC, the pattern of the VTEC fluctuations in the initial phase (16/03/2015)

Ann. Geophys. Discuss., https://doi.org/10.5194/angeo-2018-48
Manuscript under review for journal Ann. Geophys.
Discussion started: 5 June 2018

and in the recovery phase (18/03/2015) of the storm was considered. As shown in Fig. 13, the GPS-VTEC values show significant fluctuation that indicates the occurrence of storm. On the other hand, the model VTEC values (IRI 2007, IRI 2012 and IRI 2016 VTEC) don't show any change when the storm model is "on" and "off" (see Figs.13a-13c and Figs.13d-13f). As shown in the figures, the mode VTEC values in all the three days follow almost similar pattern; they generally tend to underestimate the VTEC values and remain smooth during the storm. This shows that the model does not respond to the effects resulting from storm. In addition, enhancement of GPS TEC is observed as we proceed from the initial to the recovery phase of the storm. As shown in the figure, a peak VTEC value of about 65 TECU being observed in the initial phase increases to about 75 TECU in the recovery phase of the storm. This may be resulted from particle transport and the prompt penetration of high latitude electric field to lower latitude which travel equator ward with high velocities during the storm (Malik et al., 2010; Tsurutani et al., 2004; Sobral et al., 2001).

4. Conclusions

Because of the unique geometry of the geomagnetic field near the magnetic equator and low latitude regions (such as Ethiopia), the signal propagation system through the ionosphere is largely affected by the accumulation of electrons (TEC). Hence, in this study, the VTEC variation and the improvement of performance of the IRI model over the equatorial and low latitude regions has been studied employing the GPS and IRI techniques during the period of 2013-2016. The results reveal that the monthly and seasonal highest peak hourly VTEC values are mostly observed in the equinoctial months; while the lowest peak values are observed in the June solstice months. It has also been shown that both the measured and modeled VTEC values

start increasing at about 03:00 UT or 06:00 LT and reach their peak values in the time interval of about 09:00-13:00 UT or 12:00-16:00 LT. In addition, the maximum and minimum monthly and seasonal arithmetic mean hourly VTEC values are observed in the equinoctial and June solstice months, respectively. In addition, though overestimation of the modeled VTEC has been observed on most of the hours (especially in using IRI 2016 model), the model is generally good to estimate the diurnal hourly VTEC values mostly just after midnight hours (00:00-03:00 UT or 03:00-06:00 LT). However, the model is found to generally overestimate both the arithmetic mean of the monthly and seasonal hourly VTEC values in the June solstice and September equinox months, with the highest overestimation being observed in using IRI 2016 version. On the other hand, underestimation is observed in the March equinox and December solstice months, with the highest underestimation being observed in using the same version of the model (IRI 2016 version). Moreover, the model is found to generally overestimate both the arithmetic mean of the monthly and seasonal hourly VTEC values, with the highest overestimation being observed in using IRI-2001 option. The overall results show that using NeQuick option for the topside electron density is, generally, better than other topside options for TEC estimation by IRI model. In addition, the model does not show good improvements from version IRI 2007 to IRI 2016 in the TEC estimation over equatorial and low latitude regions. All versions of the model do not also respond to the effects resulting from storm. Hence, further improvements have to be made on the model for the betterment of its performance in estimating the VTEC over the equatorial and low latitude regions.

Author contribution

All the required issues for the manuscript are prepared by the corresponding author, Yekoye

Competing interests

The corresponding author declares that he has no conflict of interest.

Acknowledgements

The data of daily sunspot number, GPS, Dst index and IRI model for this paper are freely available at: http://www.sidc.be/sunspot-data/,http://facility.unavco.org/data/dai2/app/dai2., http://wdc.kugi.kyoto-u.ac.jp/dst_final/201401/index.html and (http://omniweb.gsfc.nasa.gov/vitmo/iri vitmo.html), respectively. Hence, the author is very grateful to UNAVCO, NOAA, World Data Center (Kyoto University) and NASA for donating their free GPS, daily sunspot number, Dst index and online IRI model data, respectively.

References

Abdu, M.A., Batista, I.S.,Souza JR.(1996); An overview of IRI-observational data comparison in American (Brazilian) sector low latitude ionosphere. Adv Space Res 18(6):13-22.

Asmare Y., Tsgaye, K., Melssew, N. (2014); Validation of IRI-2012 TEC model over Ethiopia during solar minimum (2009) and solar maximum (2013) phases. Adv Space Res, 1582-1594, http://dx.doi.org/10.1016/j.asr.2014.02.017.

Bhuyan, P.K., Borah,R.R. (2007); TEC derived from GPS net work in India and comparison with IRI. Advances in Space Research: The Official Journal of the Committee on Space Research (COSPAR) 39, 830-840.

Bilitza, D. (2001); International reference ionosphere 2000. Radio Sci. 36(2), 261-275.

Bilitza, D., D. Altadill, Y. Zhang, C. Mertens, V. Truhlik, P. Richards, L. McKinnell, and

B. Bodo Reinisch, (2014); The International Reference Ionosphere 2012 – a model of international collaboration, J. Space Weather Space *Clim.*, 4, A07, DOI: 10.1051/swsc/2014004

Bilitza1, D, D. Altadill, V. Truhlik, V. Shubin, I. Galkin, B. Reinisch, X. Huang (2017**);** International Reference Ionosphere 2016: from ionospheric climate to real-time weather predictions, Space Weather, DOI: 10.1002/2016SW001593.

Chakraborty,M., Kumar, S., Kumar, B., Guha, A.(2017); Latitudinal characteristics of GPS derived ionospheric TEC: a comparative study with IRI 2012 model, Annals of Geophysics, 57 (5), A0539; doi: 10.4401/ag-6438.

Ciraolo, L., F. Azpilicueta, C. Brunini, Meza, A. and S. M. Radicella (2007); Calibration errors on experimental slant total electron content (TEC) determined with GPS, *J., Geodesy*, 81, 111–120

Ezquer, R.G., López, J.L., Scidá, L.A., Cabrera, M.A., Zolesi, B., Bianchi, C., Pezzopane M., Zuccheretti, E., Mosert, M. (2014); Behaviour of ionospheric magnitudes of F2 region over Tucumán during a deep solar minimum and comparison with the IRI 2012 model predictions. J. Atmos. Sol-Terr. Phys. 107:89-98.

Gao, Y.,Liu,Z.Z. (2002); Precise ionospheric modeling using regional GPS network data, Journal of Global Positioning system, vol. 1, No. 1:18-24.

Hansen, A., Blanch,J., T. Walter, T. (2000); Ionospheric correction analysis for WAAS quiet and stormy, in Proceedings of the 13th International Technical Meeting of the Satellite Division of The Institute of Navigation ION GPS, Salt Lake City, Utah, 19-22.

Hofmann-Wellenhof, B., Lichtenegger, H., Collins, J. (1992); Global Positioning System Theory and Practice. Springer-VerlagWien, New York.

384 Hunsucker, R.D. and Hargreaves, R.D. (2003); The high-latitude ionosphere and its effects on
385 radio propagation, Cambridge Univ. Press, UK.
386 Kakinami, Y., Liu, J.Y., Tsai, L.C. (2012); A comparison of a model using the FORMOSAT-
387 3/COSMIC data with the IRI model. Earth, Planets, Space, 64:545-551.
388 Kelley, M.C. (2009); The Earth's Ionosphere: Plasma Physics and Electrodynamics,
389 Second Edition. Elsevier Inc., New York.
390 Kumar, S., Tan, E., Murti. D. (2015); Impacts of solar activity on performance of the IRI-2012
391 model predictions from low to mid latitudes. Earth, Planets, Space, 67:42.
392 doi:10.1186/s40623-015-0205-3
393 Kumar, S. (2016); Performance of IRI-2012 model during a deep solar minimum and a
394 maximum year over global equatorial regions, J. Geophys. Res., Space Physics, 121,
395 doi:10.1002/2015JA022269.
396 Klobuchar, J.A., Parkinson, B.W., Spilker, J.J. (1996); Ionospheric effectson GPS, in: Global
397 Positioning System: Theory and Applications, American Institute of Aeronautics and
398 Astronautics,Washington, DC.
399 Lanyi, G.E. and Roth, T. (1988); A Comparison of Mapped and Measured Total Ionospheric
400 Electron Content Using Global Positioning System and Beacon Satellite Observations.
401 Radio Science, Vol. 23, No. 4, pp. 483-492.
402 Mannucci, A.J., Wilson, B.D., Yuan, D.N., Ho, C.H., Lindqwister, U.J.,Runge, T.F. (1998); A
403 global mapping technique for GPS-derived ionospheric total electron content
404 measurements. Radio Sci. 33, 565-582, http://dx.doi.org/10.1029/97RS02707.
405 Malik, Rakhee, Sarkar, Shivalika, Mukherjee, Shweta, Gwal, A.K (2010); Study of ionospheric
406 variability during geomagnetic storms. J. Ind. Geophys. Union 14 (1), 47-56.

Misra, P., Enge, P.(2006); Global Positioning System Signals, Measurements and Performance, second ed. Ganga-Jamuna Press.

Nahavandchi, H., Soltanpour, A. (2008); Local ionospheric modeling of GPS code and carrier phase observation, vol. 40,309, pp.271-284.

Nigussie, M., Radicella, S.M., Damtie, B.,Nava,B., Yizengaw, E., Groves, K. (2013); Validation of the NeQuick 2 and IRI-2007 models in East-African equatorial region. J. Atmos. Sol-Terr. Phys., http://dx.doi.org/10.1016/j.jastp.2013.04.016.

Norsuzila, Y., Ismail, M., Abdullah M. (2008); Investigation of the GPS signals ionospheric correction: Ionospheric TEC prediction over equatorial region, IEEE International Conference on Telecommunications and Malaysia International Conference on Communications (ICT-MICC 2007); Penang, Malaysia. 294-298, 14-17.

Norsuzila, Y., Mardina, A., Mohamod, I., Azami, Z. (2009); Model validation for Total electron coneten (TEC) at equatoria region, Europian Journal of scientific research vol.28, No.4, pp 642-648.

Olwendo, O.J., Baki, P., Mito, C., Doherty, P. (2012a); Characterization of ionospheric GPS total electron content (GPS TEC) in low latitude zone over the Kenyan region during a very low solar activity phase. J. Atmos. Sol-Terr. Phys., 84-85:52-61.

Olwendo, O.J., Baki, P., Mito, C., Doherty,O. (2012b); Comparison of GPS TEC variations with IRI-2007 TEC prediction at equatorial latitudes during a low solar activity (2009-2011) phase over the Kenyan region. J Adv Space Res. http://dx.doi.org/10.1016/j.asr.2012.08.001.

Rios, V.H., Medina, C.F., Alvarez, P. (2007); Comparisons between IRI predictions and digisonde measurements at Tucuman. J. Atmos. Sol. Terr. 69, 569-577..

Sobral, J. H., M. A. Abdu, C. S. Yamashita, W. D. Gonzalez, A. C. de Gonzalez, I. S. Batista, C. J. Zamlutti, and B. T. Tsurutani (2001), Responses of the low-latitude ionosphere to very intense geomagnetic storms, J. Atmos. Sol. Terr. Phys., 63, 965–974, doi:10.1016/S1364 6826(00)00197-8.

Tariku Y.A. (2015a); Patterns of GPS-TEC variation over low-latitude region (African sector) during the deep solar minimum (2008 to 2009) and solar maximum (2012 to 2013) phases. Earth, Planets, Space 67:35. doi:10.1186/ s40623-015-0206-2.

Tariku, Y.A. (2015b); TEC prediction performance of the IRI-2012 model over Ethiopia during the rising phase of solar cycle 24 (2009-2011), Earth, Planets and Space (2015) 67:140 DOI 10.1186/s40623-015-0312-1.

Tsurutani, B., et al. (2004), Global dayside ionospheric uplift and enhancement associated with interplanetary electric fields, J. Geophys. Res., 109, A08302, doi: 10.1029/2003JA010342.

Wu, C.C., Fry, C.D., Liu, J.Y., Liou, K., Tseng, C.L. (2004); Annual TEC variation in the equatorial anomaly region during the solar minimum: September, 1996-August 1997., J. Atmos. Terr. Phys., 66:199-207.

Figures

Ann. Geophys. Discuss., https://doi.org/10.5194/angeo-2018-48
Manuscript under review for journal Ann. Geophys.
Discussion started: 5 June 2018

Annales Geophysicae Discussions
Open Access
EGU

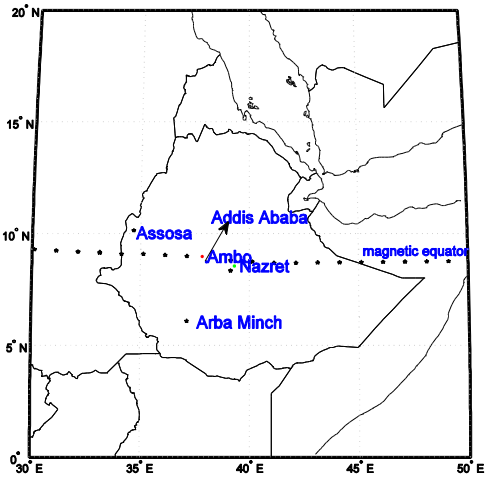

447

448 Figure 1: Location of GPS receivers used for the study

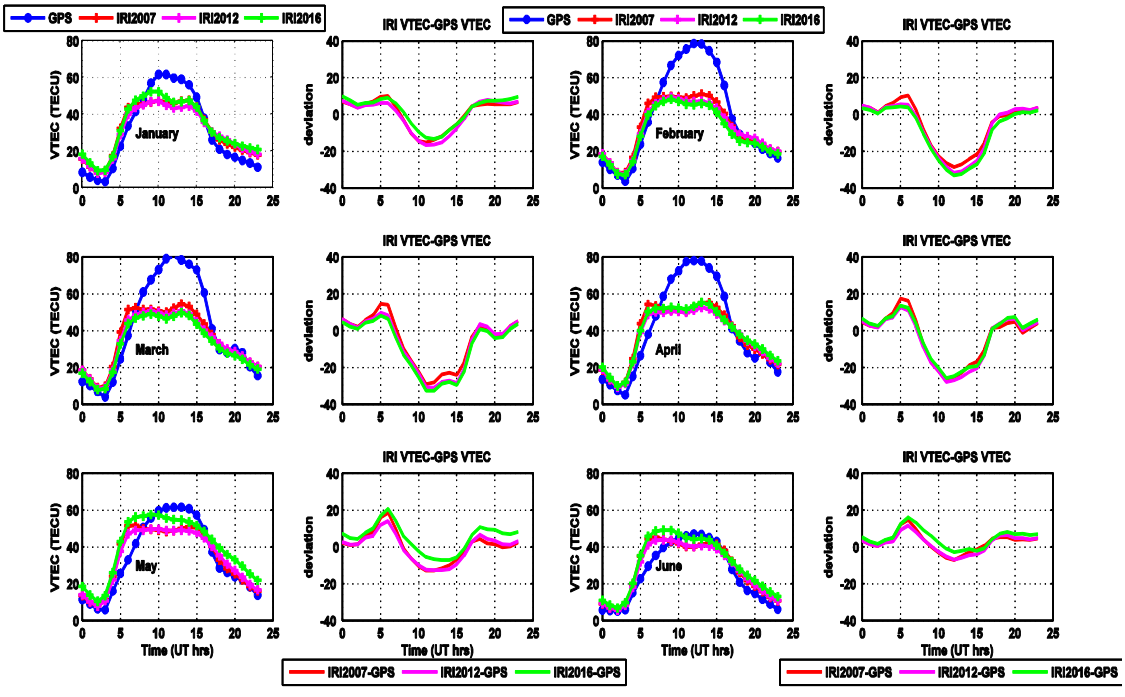

449

450 Figure 2: A graph to illustrate diurnal monthly VTEC variation and performance of the IRI

451 model over Arba Minch station during the period of January-June in 2015

Ann. Geophys. Discuss., https://doi.org/10.5194/angeo-2018-48
Manuscript under review for journal Ann. Geophys.
Discussion started: 5 June 2018

Annales Geophysicae Discussions
Open Access
EGU

452

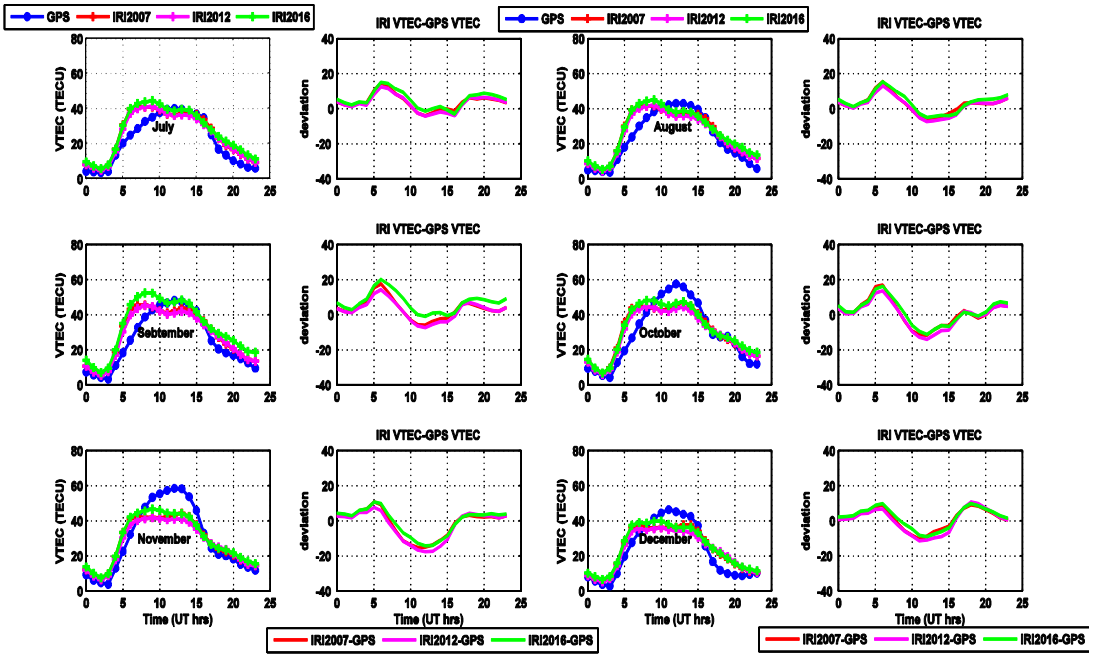

453

454 Figure 3: A graph to illustrate diurnal monthly VTEC variation and performance of the IRI

455 model over Arba Minch station during the period of July-December in 2015

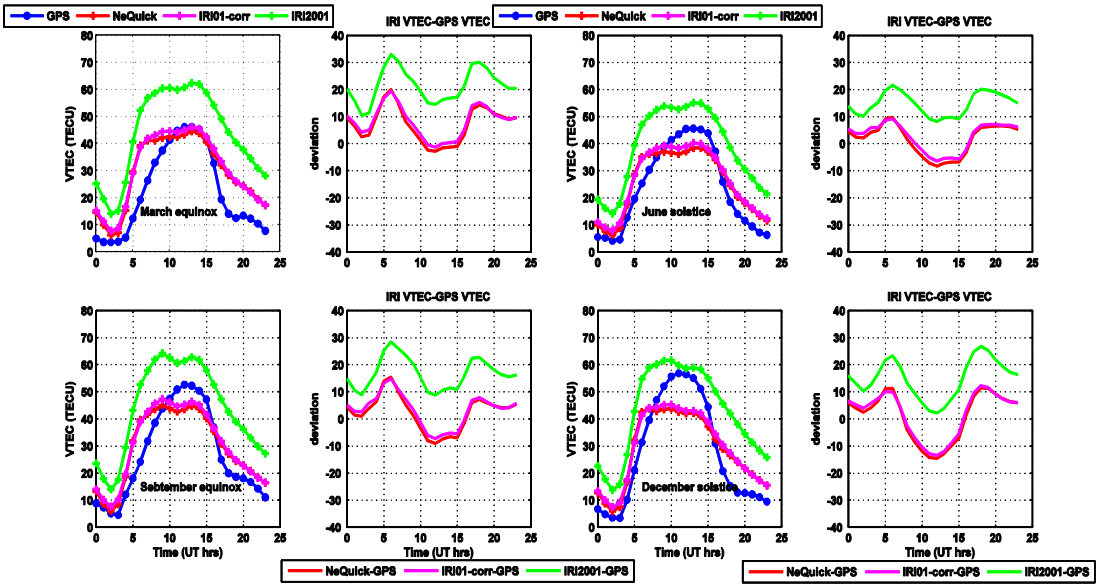

456

Ann. Geophys. Discuss., https://doi.org/10.5194/angeo-2018-48
Manuscript under review for journal Ann. Geophys.
Discussion started: 5 June 2018

457

458 Figure 4: A graph to illustrate diurnal seasonal VTEC variation and performance of the IRI-2012

459 model over Ambo station during the period of 2013

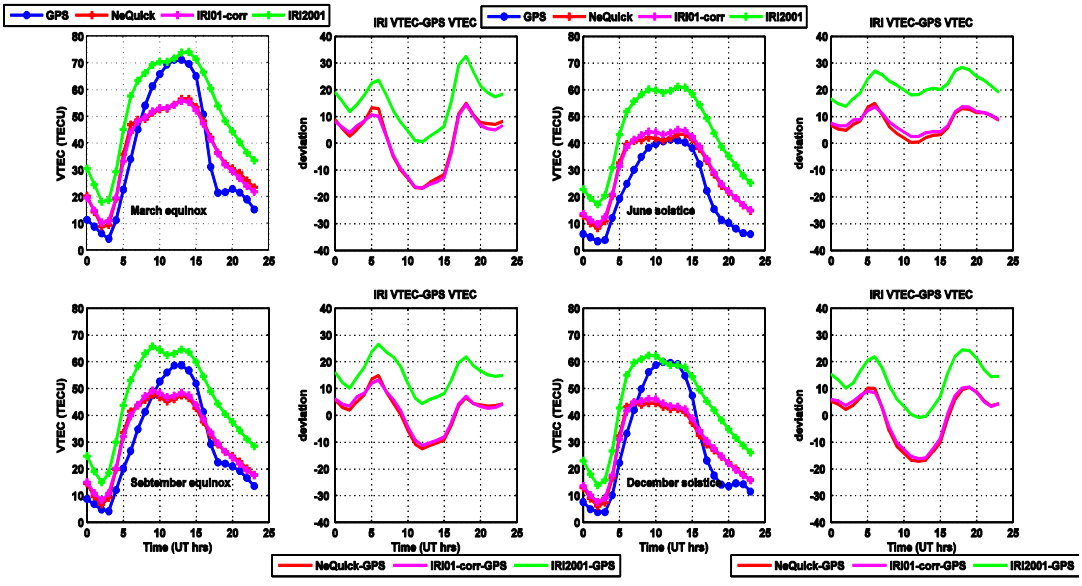

460

461 Figure 5: A graph to illustrate diurnal seasonal VTEC variation and performance of the IRI-2012

462 model over Ambo station during the period of 2014

Ann. Geophys. Discuss., https://doi.org/10.5194/angeo-2018-48
Manuscript under review for journal Ann. Geophys.
Discussion started: 5 June 2018

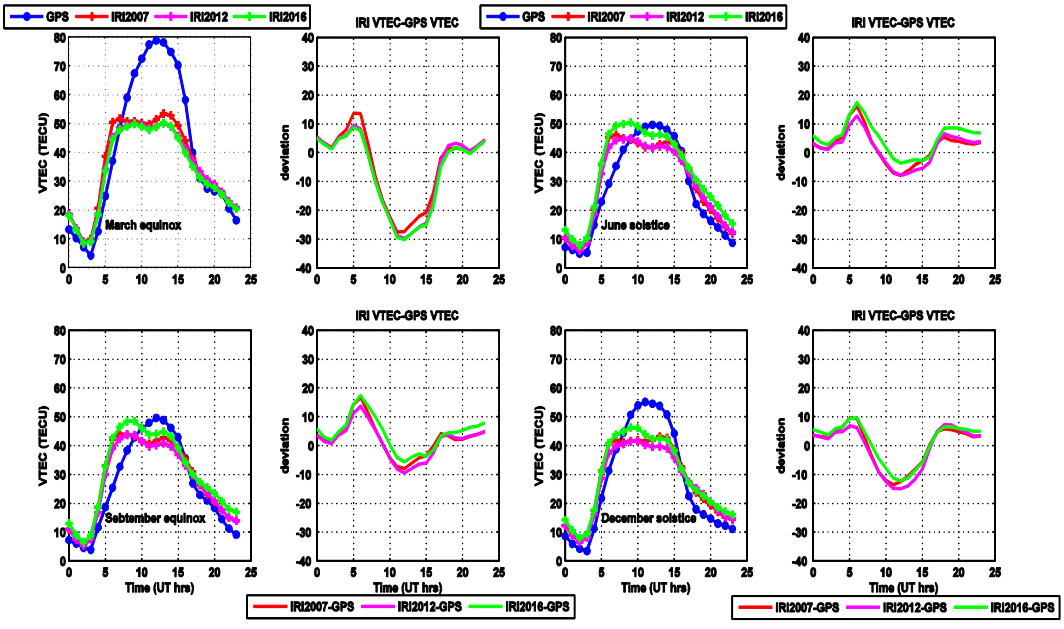

463

464

465 Figure 6: A graph to illustrate diurnal seasonal VTEC variation and performance of the IRI

466 model over Arba Minch station during the period of 2015

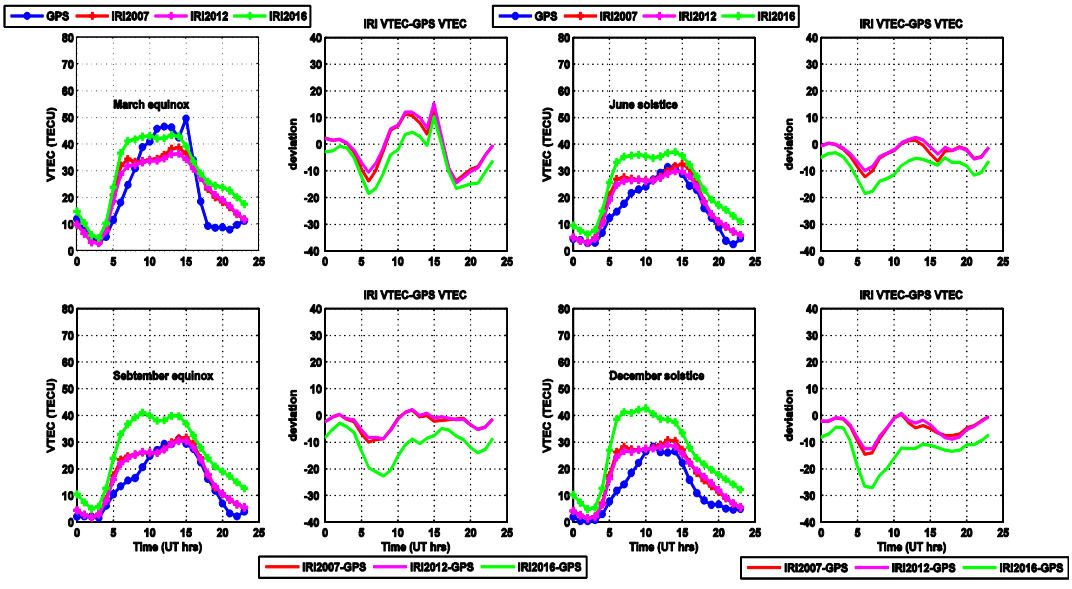

467

Ann. Geophys. Discuss., https://doi.org/10.5194/angeo-2018-48
Manuscript under review for journal Ann. Geophys.
Discussion started: 5 June 2018

Annales Geophysicae Discussions

468 Figure 7: A graph to illustrate diurnal seasonal VTEC variation and performance of the IRI
469 model over Asosa station during the period of 2016

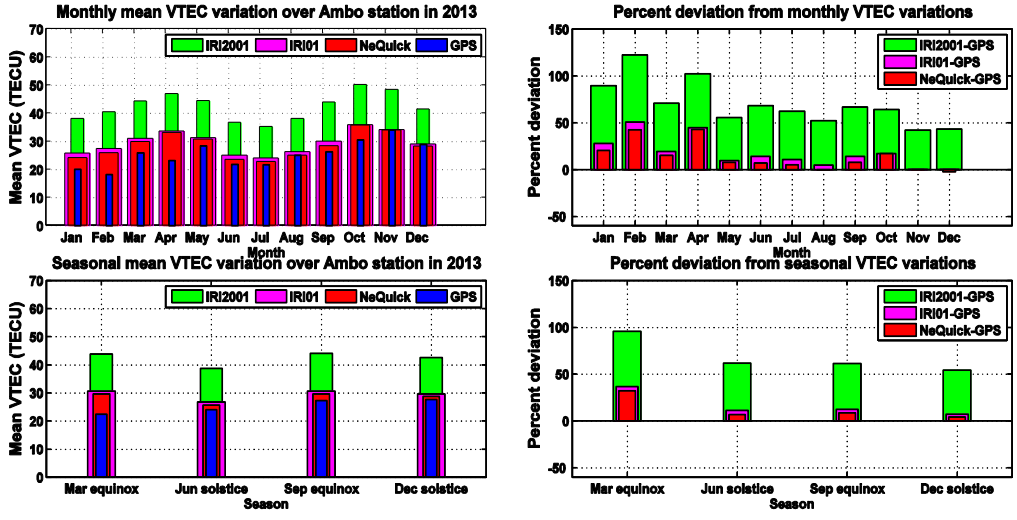

470

471 Figure 8: A graph to illustrate the arithmetic mean monthly and seasonal VTEC variation and
472 performance of the IRI-2012 model over Ambo station during the period of 2013

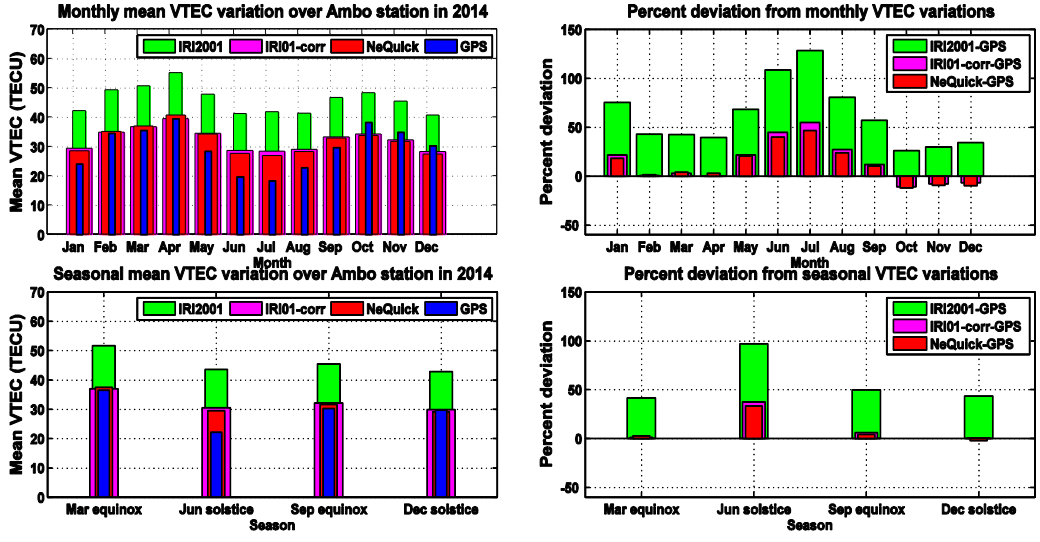

473

Ann. Geophys. Discuss., https://doi.org/10.5194/angeo-2018-48
Manuscript under review for journal Ann. Geophys.
Discussion started: 5 June 2018

Annales Geophysicae Discussions
Open Access
EGU

474 Figure 9: A graph to illustrate the arithmetic mean monthly and seasonal VTEC variation and

475 performance of the IRI-2012 model over Ambo station during the period of 2014

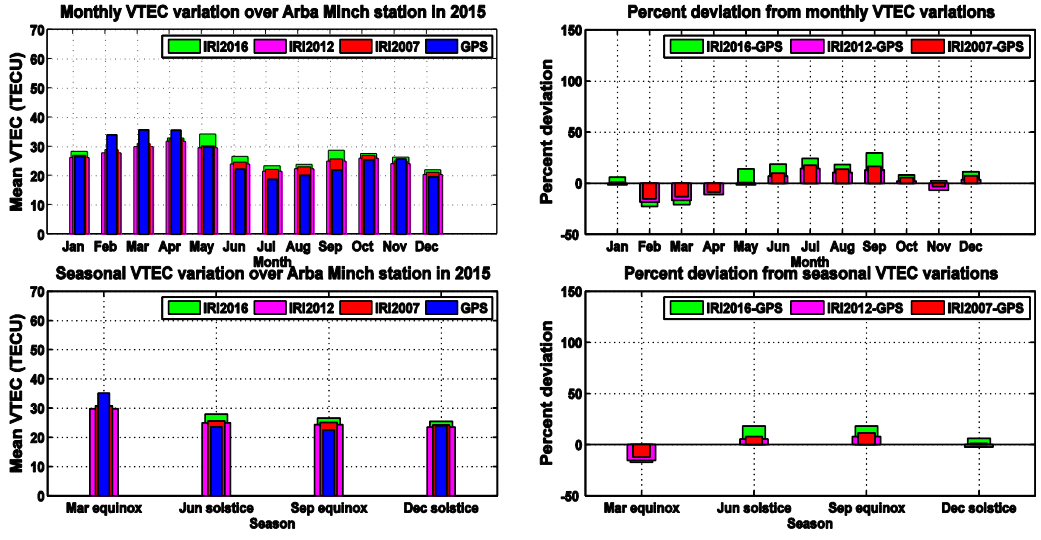

476

477

478 Figure 10: A graph to illustrate the arithmetic mean monthly and seasonal VTEC variation and

479 performance of the IRI model over Arba Minch station during the period of 2015

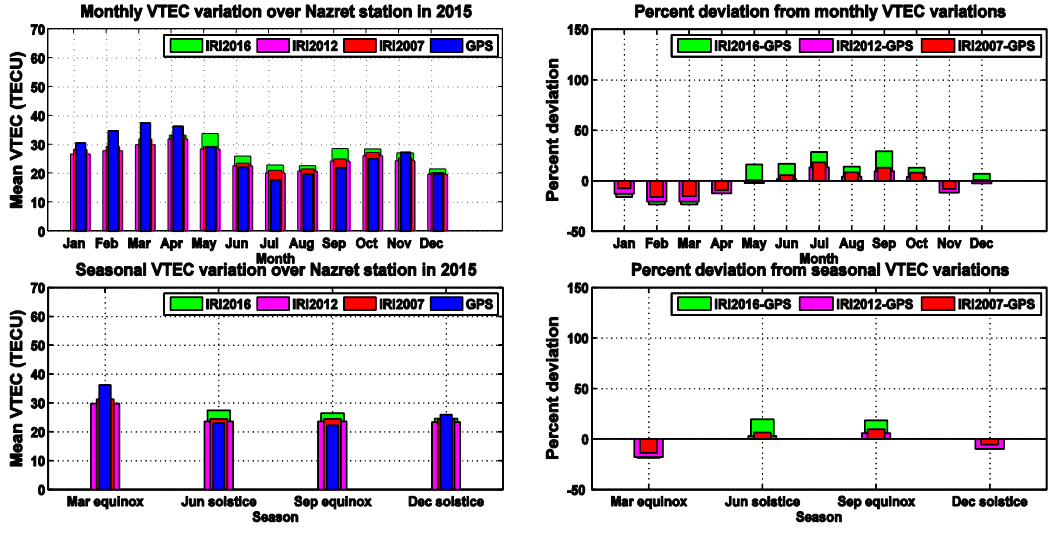

480

Ann. Geophys. Discuss., https://doi.org/10.5194/angeo-2018-48
Manuscript under review for journal Ann. Geophys.
Discussion started: 5 June 2018

481 Figure 11: A graph to illustrate the arithmetic mean monthly and seasonal VTEC variation and

482 performance of the IRI model over Nazret station during the period of 2015

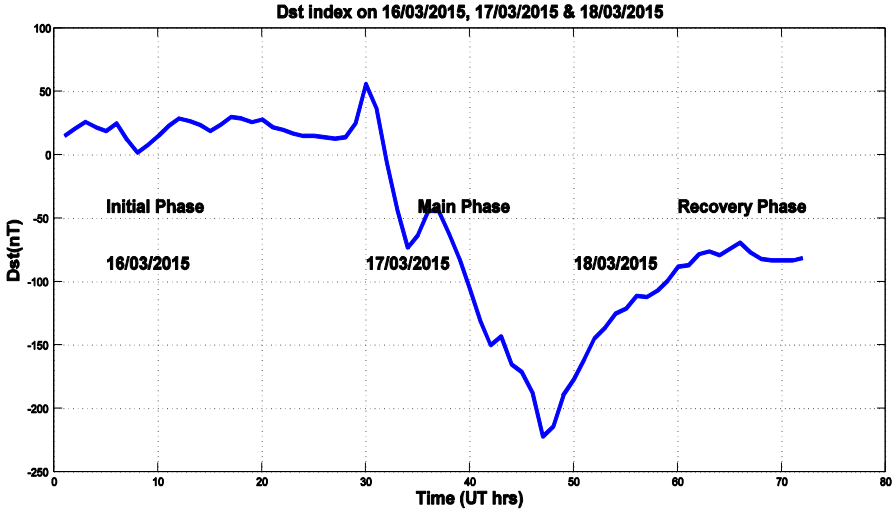

483

484

485 Figure 12: Dst index on 16/03/2015, 17/03/2015, and 18/03/2015 as observed over Arba Minch

486 station during the period of 2015 (data source for Dst index: World Data Center, Kyoto

487 University).

Ann. Geophys. Discuss., https://doi.org/10.5194/angeo-2018-48
Manuscript under review for journal Ann. Geophys.
Discussion started: 5 June 2018

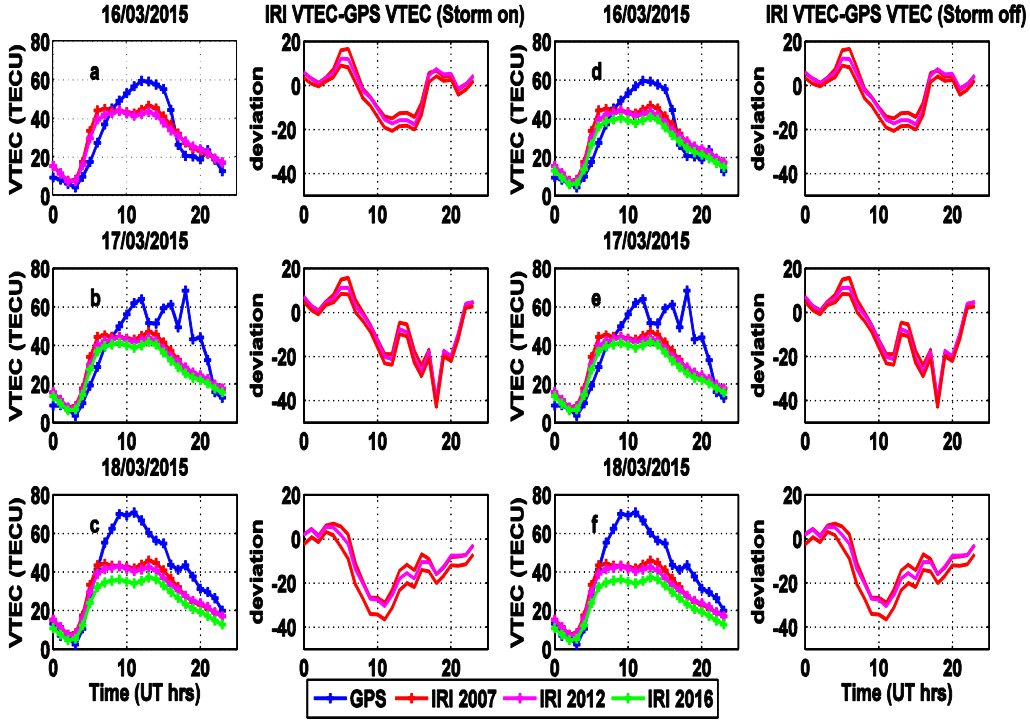

Figure 13: A graph to show the variation of the VTEC and the response of IRI model on storm time condition which occurred on March 17/2015 as observed over Arba Minch station. Figures 14a–14c and Figures 14d–14f show patterns of the modeled and measured VTEC values when the storm option is "on" and "off," respectively.

Station	code	Geographic coordinates Lat. (N), Long. (E)	Geomagnetic coordinates Lat. (N), Long. (E)
Asosa	asos	(10.05,34.55)	(0.56,106.38)
Ambo	aboo	(8.97,37.86)	(0.07,109.80)
Nazret	nazr	(8.57,39.29)	(-0.08,111.27)
Arba MInch	armi	(6.06,37.56)	(-3.08,109.57)

Table 1: Coordinates of GPS receivers used for the study